IEEE Access
Multidisciplinary ⋮ Rapid Review ⋮ Open Access Journal

Received 30 August 2022, accepted 28 October 2022, date of publication 1 November 2022, date of current version 8 November 2022.

Digital Object Identifier 10.1109/ACCESS.2022.3218702

RESEARCH ARTICLE

Multi-Aircraft Formation Recognition Method of Over-the-Horizon Radar Based on Deep Transfer Learning

FUTAI LIANG[1,2], YAN ZHOU[1], HUI LI[1], XUN FENG[1], AND JUNBIAO ZHANG[1]
[1]Air Force Early Warning Academy, Wuhan 430019, China
[2]31121 PLA Troops, Nanjing, Jiangsu 210000, China
Corresponding author: Yan Zhou (yunshanlele@sina.com)

ABSTRACT Over-the-horizon radar (OTHR) is an important equipment for the ultralong-range early warning in the military, but the use of constant false-alarm rate (CFAR), which is a traditional detection method, makes it difficult in multi-aircraft formation recognition. To solve this problem, a multi-aircraft formation recognition method based on deep transfer learning in OTHR is proposed. First, the range-Doppler images of aircraft formation in OTHR are simulated, which are composed of four categories of samples. Secondly, a recognition model based on Convolutional Neural Network (CNN) and CFAR detection technology is constructed, whose training method is designed as a two-step transfer. Finally, the trained model can well distinguish the spectral characteristics of aircraft formation, and then recognize the aircraft number of a formation. Experiments show that the proposed method is better than the traditional CFAR detection method, and can detect the number of aircraft more accurately in the formation with the same false alarm rate.

INDEX TERMS Multi-aircraft formation, range-Doppler image, OTHR, deep transfer learning.

I. INTRODUCTION

Due to its long detection distance and unique detection mechanism, over-the-horizon radar (OTHR) plays an irreplaceable role in strategic early warning and stealth target detection and has become an important part of early warning and detection system [1]. However, when multiple targets are located within OTHR antenna beamwidth and the same range unit, their number is not easy to identify [2]. In modern warfare, fighters often fly in a dense formation to interfere with the accurate judgment of radar on their target characteristics [3]. So, the multi-aircraft formation recognition of OTHR is very important for commanders to recognize the battlefield situation, which has important practical significance in future war.

At present, the multi-aircraft formation recognition of OTHR mainly depends on the difference in target Doppler frequency [4]. After receiving the target echo, the radar obtains the range-Doppler-amplitude spectrum of the target through range-Doppler processing and then uses constant false-alarm rate (CFAR) processor to detect and recognize the multi-aircraft formation [5]. The wide aperture receiving antenna array of OTHR can obtain high azimuth resolution, but the horizontal range and vertical range of the detection region reach the same order of magnitude due to its long detection distance. When there are multiple targets in the same distance unit, the noise estimation in the reference window is high due to the spectral peak broadening and spectral peak adhesion caused by multi-target aggregation, which reduces the ability to find adjacent weak targets and makes it difficult to detect and recognize multi-aircraft formation only by Doppler velocity resolution [6].

To solve the above problems in multi-aircraft formation recognition, a lot of research has been done in two aspects. One is to improve CFAR detection method, the other is to extract spectral characteristics of aircraft formation. In terms of CFAR detection method, in addition to the improved traditional cell averaging CFAR (CA-CFAR), ordered statistics CFAR (OS-CFAR), and adaptive CFAR methods, the use of neural network and support vector machine (SVM) classification algorithm is studied to classify and distinguish the clutter

The associate editor coordinating the review of this manuscript and approving it for publication was Baozhen Yao.

background and then select the appropriate CFAR method according to the classification results [7], [8], [9], [10], [11]. However, in practical application, these methods still need to estimate the distribution of clutter in advance, which is related to the selection of the distribution model and the setting of the reference cell, and result in many disadvantages for multi-aircraft formation recognition. In terms of the spectral characteristics of aircraft formation, the method of increasing the dimensions of the target characteristic is proposed to increase the multi-target detection accuracy [12]. A multi-target detection method and adaptive waveform design algorithm are studied, which significantly improves the performance of multi-target detection [13]. The clustering algorithm of density-based spatial clustering of applications with noise and k-nearest neighbor (k-NN) are used to classify targets after the multi-target features extraction [14]. A method to decompose the multi-targets information on the RV plane for effective multi-target classification is proposed [15], and so on. However, due to the inherent defects of the low-resolution radar itself, the methods in the literatures mentioned above still have some limitations in the target detection of OTHR, such as the difficulty of target spectrum feature extraction, the great influence of subjective factors on the feature extraction rules, and the difficulty in ensuring the effectiveness of feature extraction.

Target detection and recognition technology based on deep learning is a target detection technology developed from convolutional neural network technology. Compared with traditional target detection technology, it shows greater performance advantages and has been widely used in the military and civil fields. Due to the unique advantages of deep learning technology in image feature extraction, relevant studies have adopted the method of deep learning to detect and recognize many sorts of targets such as airplanes, ships, and soon on [16], [17]. Using deep learning technology can automatically extract multi-level target spectrum features, and avoid the interference and information loss caused by human factors. But its disadvantage is also prominent, which is that it needs a large number of tens of thousands of labeled data to train the model [18]. In the practice of air defense early warning, acquiring and labeling aircraft formation spectrum data are difficult, which means it is also hard to recognize multi-aircraft formation by directly using deep learning method.

In this paper, a multi-aircraft formation recognition method based on range-Doppler image and deep transfer learning is proposed, which realizes multi-target formation recognition of OTHR. Specifically, the contributions of this paper are as follows:

1) A recognition model based on Convolutional Neural Network (CNN) and CFAR is designed. If the CFAR detector is used alone, the multi-target is not easy to recognize. To solve this problem, CNN is added after CFAR processing to overcome the problem of low accuracy of traditional CFAR detection methods in multi-target formation recognition.
2) The model training method is designed as a two-step transfer, which not only solves the problem that it is difficult to apply deep learning technology with insufficient real measured data but also further improves the recognition accuracy of the model. Compared with the one-step transfer method, the two-step transfer method uses a dataset closer to the real measured data to train the recognition model and achieves better results.
3) According to the characteristics of multi-target formation, we propose a special data augmentation method, which expands the scale of real measured data and lays a foundation for model training. Compared with the traditional augmentation method in the training process of deep learning, the proposed method is more suitable for this task.

The rest of this paper is organized as follows. Section 2 introduces the framework of the method and some concepts involved. Section 3 describes the dataset generating and model turning in detail. Section 4 illustrates and analyzes experimental results, and the conclusions are given in Section 5.

II. METHODOLOGY

The multi-aircraft formation is not easy to distinguish from one target by the traditional CFAR detection method. However, practical experience shows that there are some differences in the characteristics of the echo spectrum between multi-aircraft and single target, and experienced operators can effectively distinguish these differences. Deep learning technology has a good application in the visual application [19], so applying deep learning technology to multi-aircraft recognition will achieve good results. There is no need to calculate statistics or other parameters in the recognition based on deep learning method, while only need the classifier network trained to automatically recognize the subtle differences of spectral features in the range-Doppler image. But a large number of labeled data is needed to achieve better results in deep learning method. In the practice, it is difficult to collect a large number of measured data. Luckily, deep transfer learning technology can solve the problem with small sample size well.

A. THE METHOD FRAMEWORK

A multi-aircraft formation recognition method based on deep transfer learning is proposed in this section. In this method, a model combining CFAR and CNN is designed to extract the deep features of target relevant cells and classify them, so as to realize the recognition of multi-aircraft formation and avoid various problems caused by CFAR detection method and manual interpretation. The method framework is shown in Fig.1.

According to the signal flow of OTHR for the multi-aircraft formation recognition shown in Fig.1, when receiving the target echo, an OTHR will generate a range-Doppler-amplitude image (also called range-Doppler image) after signal

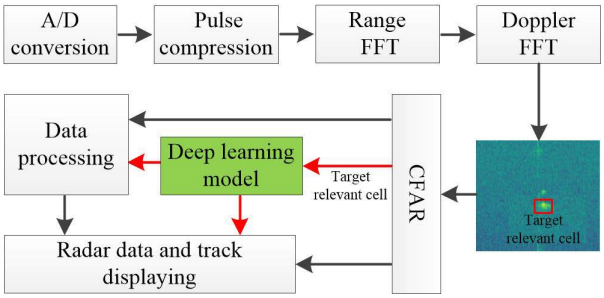

FIGURE 1. Framework of the proposed method.

processing, which includes digital conversion, pulse compression, and 2D fast Fourier transforms (FFT) [20]. Then, the range-Doppler image is sent into CFAR processing channel, in which the target will be detected through typical CFAR detection and the target position will be used to determine target relevant cells, which are the cells around the target position. Next, the target relevant cells are inputs to the deep learning model for classification and recognition, and the recognition result of the target number in the aircraft formation is obtained. Finally, the recognition results acquired from the CFAR and deep learning model are respectively sent to the data processing unit for subsequent processing and the output terminal for track display.

In Fig.1, the deep learning model is pre-trained by the training dataset. The model training method of the two-step transfer is designed to solve the small sample size problem of real measured data. This training method is also helpful to improve the accuracy of multi-aircraft formation recognition. The training process of the deep learning model is shown in Fig.2.

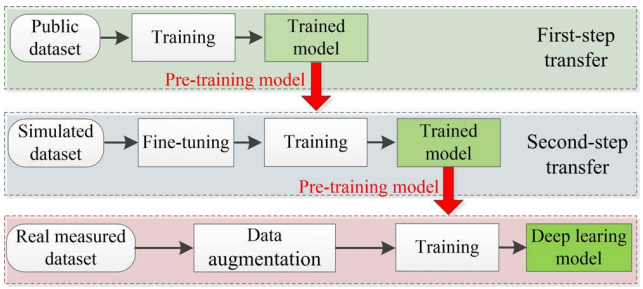

FIGURE 2. Flow of deep-learning model transferring.

The training process of the deep-learning model includes two steps, that is, first-step transfer stage and second-step transfer stage. In the first-step transfer stage, the model trained in ImageNet dataset is loaded into the deep-learning network as a pre-trained model, and then trained to obtain new model parameters as the pre-trained model for the second-step training. In the second-step transfer stage, the real data is first augmented to increase its diversity and avoid model overfitting. Then, the network model parameters obtained by first-step transfer are loaded as a pre-training model for training, the desired deep learning model is obtained after training, which can be used for real-time multi-aircraft formation recognition by deploying it in the framework of Fig.1.

B. DEEP TRANSFER LEARNING

Transfer learning is a machine learning method that uses existing knowledge to solve the task in different but related fields [21]. Transfer learning using deep neural networks is called deep transfer learning [22]. Compared with traditional transfer learning, deep transfer learning can automatically extract more expressive features and can realize end-to-end applications [23].

Transfer learning involves the concept of the domain, which include the source domain and target domain. The domain transfer is the source domain, denoted by $\mathcal{D}_\mathrm{s}$, and the domain to be learned is the target domain, denoted by $\mathcal{D}_\mathrm{t}$. Given a source domain $\mathcal{D}_\mathrm{s}$ and a target domain $\mathcal{D}_\mathrm{t}$, the purpose of transfer learning is to learn the conditional probability distribution $P(y_t\,|\boldsymbol{x}_t)$ in the domain $\mathcal{D}_\mathrm{t}$ from the domain $\mathcal{D}_\mathrm{s}$. It also is called the target prediction function $f_t(\cdot)$.

Given the source domain $\mathcal{D}_\mathrm{s} = \{(\boldsymbol{x}_{\mathrm{s}_i}, y_{\mathrm{s}_i})\}_{i=1}^{n_\mathrm{s}}$, n_s is the total number of samples in the sample space $\mathcal{X}_\mathrm{s}$ of the source domain, $\boldsymbol{x}_{\mathrm{s}_i} \in \mathcal{X}_\mathrm{s}$ is the i-th sample, and y_{s_i} is the corresponding label. For the target domain $\mathcal{D}_\mathrm{t} = \{(\boldsymbol{x}_{\mathrm{t}_i}, y_{\mathrm{t}_i})\}_{i=1}^{n_\mathrm{t}}$, n_t is the total number of samples in the sample space $\mathcal{X}_\mathrm{t}$ of the target domain, $\boldsymbol{x}_{\mathrm{t}_i} \in \mathcal{X}_\mathrm{t}$ is the i-th sample, and y_{t_i} is the corresponding label. $f \in \mathcal{H}$ is the target prediction function, and $\mathcal{H}$ is all the hypothesis spaces that satisfy the target prediction function. Then, followed structural risk minimization (SRM), the objective function of transfer learning can be formally expressed as below [24],

$$f^* = \arg\min_{f\in\mathcal{H}} \frac{1}{n_\mathrm{s}} \sum_{i=1}^{n_\mathrm{s}} \ell\left(f(\boldsymbol{x}_{\mathrm{s}_i}), y_{\mathrm{s}_i}\right) + \lambda R\left(\mathrm{T}(\mathcal{D}_\mathrm{s}), \mathrm{T}(\mathcal{D}_\mathrm{t})\right) \tag{1}$$

where $\ell(\cdot,\cdot)$ is the loss function, λ is the weight coefficient to measure the two parts, $R(\cdot,\cdot)$ is the transfer regularization term that is the complexity measure of the model, which formally equals the regularization term of SRM. $\mathrm{T}(\cdot)$ is the feature transformation function acting on the source domain and the target domain. For the network-based deep transfer learning method used in this paper, the transfer regularization term can be described as

$$R\left(\mathrm{T}(\mathcal{D}_\mathrm{s}), \mathrm{T}(\mathcal{D}_\mathrm{t})\right) R\left(\mathcal{D}_\mathrm{t}; f_\mathrm{s}\right) \tag{2}$$

and the goal is using the prediction function f_s induced from $\mathcal{D}_\mathrm{s}$ to regularize and fine-tune the target domain samples. In this paper, the regularization term adopts $\|f\|_t^2$, which is squared norm of f in $\mathcal{D}_\mathrm{t}$.

Transfer learning does not require the same distribution of the source domain and the target domain. When the model is trained in the target domain, the knowledge that has been extracted from the data and features of the source domain can be used to achieve reuse and transfer between similar or related domains [24]. Transfer learning makes the traditional learning from scratch becomes cumulative learning, which

reduces model training overhead and improves the effect of deep learning. Transfer learning enables the large-scale application of deep learning even when lacking sufficient available labeled data, which is suitable for multi-aircraft formation recognition of OTHR. In the first-step transfer stage of proposed method, the ImageNet dataset is the source domain and the simulated dataset is the target domain, in the second-step transfer stage, the simulated dataset is the source domain and the real measured dataset is the target domain.

In the framework of the multi-aircraft formation recognition method proposed, the 'pre-training + fine-tuning' paradigm, which is commonly used in the network-based deep transfer learning method, is used to realize the transfer. Network-based deep transfer learning reuse part of the network pre-trained in the source domain, including its network structure and connection parameters, then transfers it to the deep neural network used in the target domain [25]. The sketch map of network-based deep transfer learning is shown in Fig.3.

As can be seen from Fig.3, firstly, the deep learning network model is trained using a large-scale training dataset in the source domain. Then, the pre-trained part of the network in the source domain is transferred to the target domain, that is, the trained deep learning model can be used in the target domain.

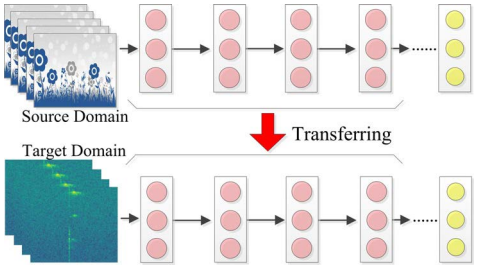

FIGURE 3. The sketch map of network-based deep transfer learning.

In general, transfer learning via multi-source data sets is necessary. It can reduce time consumption and be helpful to enhance and enrich the ability of feature extraction on target data set. But traditional transfer learning is difficult to do it. To solve this issue, Huang et al. [26] proposed a transitive transfer-based method with domain adaptation to decrease the discrepancy between the source and target tasks. Zhao et al. [27] proposed a framework named multi-source deep transfer learning (MS-DTL) that performs better than the benchmarks on the classification tasks of the small-scale hyperspectral images (HSIs).

At present, many excellent CNN models have been reused to complete many applications of deep transfer learning, such as LeNet, AlexNet, VGG, ResNet, etc.

III. DATA AND MODEL

Generating a training dataset and constructing a network model are two important steps of deep learning, and deep transfer learning is no exception.

A. DATASET ESTABLISHING

The range-Doppler images of aircraft formation are simulated according to the signal processing flow of OTHR, and then the simulation dataset is established.

1) RANGE-DOPPLER IMAGE SIMULATION

OTHR adopts frequency modulated continuous wave (FM/CW) system. The signal processing mainly includes pulse compression, Doppler processing, target detection, and so on [28]. The proposed method is based on the radar range-Doppler image and applies image recognition technology, so only the process of frequency mixing, pulse pressure, and coherent accumulation is required.

In a single chirp, the transmit signal is expressed as follows [17].

$$S_t(t) = A_t \exp\left(j2\pi\left(f_c t + \frac{B}{2T_s}t^2\right)\right) \quad (0 \le t < T_s) \tag{3}$$

where A_t is the transmit signal amplitude, f_c is the signal carrier frequency, B is the bandwidth of the chirp, and T_s is the time of the chirp.

The signal will be reflected when it meets a target. Once the reflected signal is received, after mixing and ignoring the special small items, the received signal can be expressed as

$$S_m(t) \approx A_m \exp\left(j2\pi\left(f_c\frac{2R_0}{\mathrm{c}} + \left(\frac{2BR_0}{T_s\mathrm{c}} - \frac{2f_c v}{\mathrm{c}}\right)t\right)\right) \quad (0 \le t < T_s) \tag{4}$$

where A_m is the amplitude of the mixing signal, R_0 is the distance between the target and the radar at time $t = 0$, c is the speed of light, and v is the radial running speed of the target relative to the radar.

The transmitter repeatedly sends out M chirp signals, then the echo signal after mixing can be written as

$$S_m(\hat{t}, t_m) \approx A_m \exp\left(j2\pi\left(f_c\frac{2(R_0 + vt_m)}{\mathrm{c}} + \left(\frac{2B(R_0 + vt_m)}{T_s\mathrm{c}} - \frac{2f_c v}{\mathrm{c}}\right)\hat{t}\right)\right) \quad (0 \le \hat{t} < T_s, 0 \le \frac{t_m}{T_s} < M) \tag{5}$$

where $\hat{t}$ is the fast time, measuring the transmission time of the signal, and t_m is the slow time, measuring the start time of each chirp signal.

Sampling a chirp signal, the number of sampling points is N, then the mixed signal can be expressed as a $N \times M$ matrix, and the matrix elements are

$$S_m(n, m) \approx A_m \exp\left(j2\pi\left(f_c\frac{2(R_0 + vmT_s)}{\mathrm{c}} + \left(\frac{2B(R_0 + vmT_s)}{T_s\mathrm{c}} - \frac{2f_c v}{\mathrm{c}}\right)\frac{T_s}{N}n\right)\right) \quad (0 \le n < N, 0 \le m < M) \tag{6}$$

where n is the fast time sample index, and m is the chirp signal index.

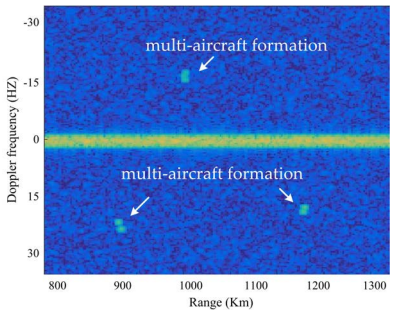

FIGURE 4. Simulated range-doppler image.

The range-Doppler response of the target can be obtained by two-dimensional Fourier transform of the $N \times M$ matrix, and the range-Doppler image can be obtained by visualizing. Fig.4 is a simulated range-Doppler image. The spectrum of the aircraft formation composed of three multi-aircraft formations.

2) MULTI-AIRCRAFT FORMATION SIMULATION

In the process of aircraft formation simulation, the multipath effect is a problem that must be considered.

Because of the special detection mechanism of OTHR, the real measured data often has the multipath effect [29]. In the radar range-Doppler image, such as Fig.5(a), there are adjacent spectrum color blocks around the same or similar speed (Doppler) unit of the target. The area and shape of the color block are similar to the target color block, but the color is slightly light. The appearance of the multipath effect is related to the location of the target, the reflection ability of the ionosphere, and other factors. It is difficult to eliminate through the signal processing method, and it cannot be completely avoided. In the process of image-based processing, it is very easy to misjudge the target, so it must be taken into account when producing training datasets.

Because the ionospheric factors closely related to multipath are difficult to simulate, it is not realistic to simulate the target range-Doppler image with the multipath effect through signal processing. Considering that in this scenario, the research is based on images, so the complex mechanism is not discussed. In order to simplify the problem, only the statistical characteristics of the target multipath effect in the range-Doppler image are simulated here. According to the observation of the real measured data, the characteristics of the target multipath effect are extracted, and then the feature is statistically analyzed to simulate the multipath effect of the target.

In this paper, the two main features of spectral color block caused by multipath in the range-Doppler image, that is, the color block number X_{e} and color block amplitude X_{a} are extracted. The probability of random variable X_{e} is

$$P(x_e) = \begin{cases} 0.36, & x_e = 1 \\ 0.42, & x_e = 2 \\ 0.21, & x_e = 3 \end{cases} \tag{7}$$

where x_e is the value of X_e, 1, 2, and 3 represent the number of color blocks respectively. When $x_e = 1$, it means that there is no multipath effect and the color block belongs to the real target.

Assuming that X_{a1} is the amplitude of the real target spectral color block, X_{a2} is the amplitude of the spectral color block adjacent to the real target spectral color block in the multipath effect, and X_{a3} is the amplitude of the spectral color block far away from the real target spectral color block. When $X_{\mathrm{a1}} = x_{\mathrm{a1}}$, the conditional probability densities of X_{a2} is

$$f(x_{\mathrm{a2}} \,|x_{\mathrm{a1}}) = \begin{cases} \dfrac{1}{x_{\mathrm{a1}}}, & 0 < x_{\mathrm{a2}} < x_{\mathrm{a1}} \\ 0, & \text{otherwise} \end{cases} \tag{8}$$

where x_{a1} is given by the real measured data.

When $X_{\mathrm{a2}} = x_{\mathrm{a2}}$, the conditional probability densities of X_{a3} is

$$f(x_{\mathrm{a3}} \,|x_{\mathrm{a2}}) = \begin{cases} \dfrac{1}{x_{\mathrm{a2}}}, & 0 < x_{\mathrm{a3}} < x_{\mathrm{a2}} \\ 0, & \text{otherwise} \end{cases} \tag{9}$$

In this paper, the spectral color block of the target is shifted on the front and rear range unit of the target according to the probability of equation (7), and the color intensity is simulated by Monte Carlo method according to equation (8) and equation (9). Fig.5 (b) is the multipath effect simulation of two targets in a range-Doppler image.

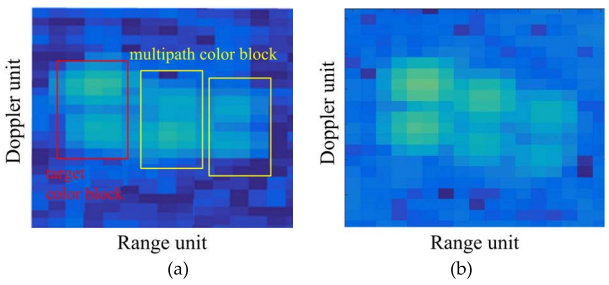

FIGURE 5. Multipath Effect. (a) The real measured image. (b) The simulated image.

The multi-aircraft formation data is generated according to the methods of multipath effect simulation and range-Doppler image simulation, and then the generated data is labeled to establish the simulation dataset. For multi-aircraft formation recognition, identifying the specific number of aircraft in a formation is the most ideal result. Due to the large range measurement error of OTHR, the difference between different targets in the range dimension can be ignored. According to the statistical analysis of target radial velocity difference in the measured multi-aircraft formation data and combined with radar technique parameters, four classes of data are generated by simulation. Each class of data is marked with digital labels 1, 2, 3, and 4, representing a formation of one, two, three and more than four aircrafts respectively.

The dataset consists of 20000 images simulated. Each image belongs to one of 4 classes. The number of images per class is 5000.

B. DATA AUGMENTATION

In the process of generating the real measured dataset, it is very important to do data augmentation.

The most important problem in the establishment of real measured datasets is that the amount of data is too small. The reason is that the collection and labeling of real measured data require manual participation, and the experience requirements of operators are high, so it is extremely difficult to collect a large amount of labeled real data. In order to avoid the problem of model overfitting in the case of a small sample size, data augmentation must be performed on the real measured data to improve the generalization ability of the model [30]. For the data of target relevant cells cut from the range-Doppler image, the data augmentation methods mainly include amplitude transformation, size transformation, and position transformation.

The amplitude transformation is to raise and lower the target spectrum amplitude to simulate the influence of target RCS, range, radar parameter setting, and other factors on the range-Doppler spectrum of OTHR. Only the influence of the target RCS is considered here.

At the same distance R, radar transmitting power P_t, antenna gain G, and receiving area A_e, the receiving power is

$$P_r = \frac{P_t G A_e \sigma}{(4\pi)^2 R^4} \tag{10}$$

where σ is used to represent the target RCS. According to equation (10), the target RCS is directly proportional to the echo power. The echo power is related to the spectral amplitude of the target in the range-Doppler image. so, by adjusting the amplitude of the target spectrum, the influence caused by the change of the target RCS can be simulated and the amount of data can be expanded.

Because the size of the general air target is close to the wavelength of OTHR. This means that they are in the resonant scattering region, the RCS of the target is greatly affected by working frequency, azimuth, pitch, and polarization. Accordingly, the target spectrum amplitude also changed greatly in the range-Doppler image. In this paper, the amplitude change is set between -5 and 5 times, and the simulation data is generated by sampling according to the uniform distribution in this interval.

The size transformation is to appropriately expand and stretch the target spectrum to simulate the influence of radar parameter setting and other factors on the range-Doppler spectrum of OTHR.

In the practical application of OTHR, according to the mission requirements and ionospheric changes, radar parameters such as pulse accumulation number need to be continuously adjusted to improve the detection rate. Accordingly, the target spectrum image size changed in the range-Doppler image. By widening and stretching, the influence caused by the change of radar parameters can be simulated and the amount of data can be expanded.

Assuming that the target spectrum Doppler-dimension transformation magnification is a random variable X_d, and the target spectrum range-dimension transformation magnification is a random variable Y_r. D is a bounded region formed by the ranges of X_d and Y_r. The two-dimensional random variable (X_d, Y_r) has a probability density function

$$f(x_d, y_r) = \begin{cases} \dfrac{1}{S(D)}, & (x_d, y_r) \in D \\ 0, & otherwise \end{cases} \tag{11}$$

where $S(\cdot)$ is the function for calculating area. Through statistical analysis, the bounded area $D : 0 \le x_d \le 3, 0 \le y_r \le 3$ is set.

The position transformation is to offset the target spectrum image to simulate the cutting deviation of the target spectrum image caused by the measurement error. Due to measurement error and other factors, the real target is often not in the center of the target relevant cells.

Let the target spectrum Doppler dimension position offset magnification be a random variable X_w, and the target spectrum distance dimension position offset magnification as a random variable Y_h. When $E(X_w) = \mu_1$, $E(Y_h) = \mu_2$, $D(X_w) = \sigma_1^2$ and $D(Y_h) = \sigma_2^2$, two-dimensional random variable (X_w, Y_h) have the probability density function

$$f(x_w, y_h) = \frac{1}{2\pi\sigma_1\sigma_2} \exp\left(-\frac{1}{2}\left(\frac{(x_w-u_1)^2}{\sigma_1^2} + \frac{(y_h-u_2)^2}{\sigma_2^2}\right)\right) \tag{12}$$

According to the actual data, we can get $\mu_1 = 0.1$, $\mu_2 = 0.2$, $\sigma_1 = 0.3$ and $\sigma_2 = 0.5$.

Using Monte Carlo simulation method, 50 sample images of each class of original data be expanded to 200 through amplitude transformation, size transformation, and position transformation. Data augmentation is programmed by calling OpenCV Library in Python language.

C. MODEL TUNING

Two steps of transfer learning are adopted in the algorithm of this paper, both of which are network-based transfer methods.

In deep transfer learning, the network-based transfer usually adopts a 'pre-training and fine-tuning' paradigm [31]. This paradigm refers to training a model with strong generalization ability on a large data set and training it as the initial parameter value of the downstream task model, so as to make the downstream task obtain a good classification effect. The 'pre-training and fine-tuning' paradigm determines whether the model structure needs to be changed according to the downstream task. In view of the fact that the source domain training dataset and the target domain training dataset are of different classes and different distributions in the first-step transfer stage, the rear layer of the original model is redesigned to make the model better for the deep-level features of the aircraft formation spectrogram. Meanwhile, the number of output categories of the output layer is made consistent with the classification number of the real measured

dataset. Since the source domain training dataset is the same as the target domain training dataset during the second-step transfer period in this paper method, no changes are made to the model structure here. Only the values of model parameters obtained by the first-step transfer period are used as the initial values, and the model is fine-tuned and trained with a small learning rate. The second-step transfer mode is simple and easy to use. Therefore, this paper mainly introduces the tuning process of the network model during the first-step transfer stage.

The deep transfer learning model can be adjusted and constructed based on the existing common models [18]. Because of its balanced performance, fewer parameters, and faster response speed, Resnet18 model is applied to the method in this paper. Retain the front layer of the model to extract the shallow features of the image, reconstruct the back two layers of the convolution layer and full connection layer, and classify these features through the full connection layer to distinguish the target echo image. Fig.6 shows the model structure.

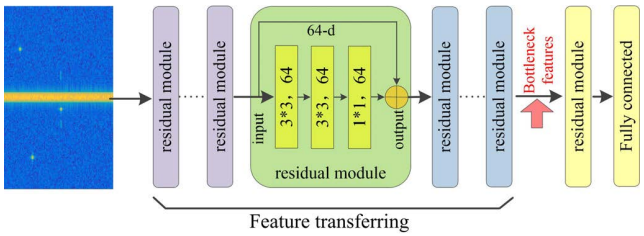

FIGURE 6. Deep transfer learning model structure.

As shown in Fig.6, the output of the bottleneck layer of the model is the feature extracted by the new transfer learning model, and the 'bottleneck feature' position is the output position of the image feature. After the reconstructed convolutional neural network obtains deep-level features, the feature vector is input into a fully connected layer for classification. The model of the fully connected layer of the transfer learning model is shown in Fig.7. We can see that there are 512 neurons on the left, corresponding to the feature vectors output by the bottleneck layer of the model, and four outputs on the right, corresponding to four classes of results: one target, two targets, three targets, and multiple targets in a formation.

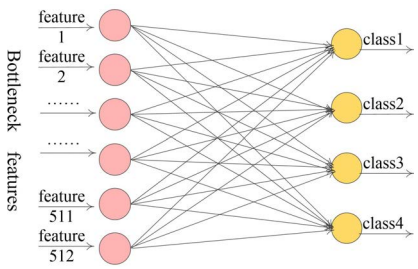

FIGURE 7. Fully connection layer structure.

IV. EXPERIMENTAL VERIFICATION

In order to verify the effectiveness and practicability of the proposed method, the two stages of transfer and two learning modes are tested and compared. Finally, we compare the proposed method with the traditional CFAR detection method.

A. EVALUATION INDICATORS

After the CFAR processing of the range-Doppler image, the preliminary detection of the target is obtained, and then the spectrum characteristics of the target area are identified by CNN, which is a classification problem.

The evaluation indexes of the classification task include accuracy rate, recall rate, precision rate, F1-score, etc., which could be intuitively expressed by drawing a confusion matrix. The recall rate, accuracy rate, and F1-score can be calculated by using the confusion matrix.

Accuracy rate (accuracy) is the ratio of the number of all correctly classified samples to the number of all samples. This is expressed as follows.

$$Accuracy = (TP + TN)/(P + N) \tag{13}$$

where TP is the number of samples that are classified as positive in the positive samples, TN is the number of samples that are classified as negative in the negative samples, P is the number of positive samples, and N is the number of negative samples. Accuracy is generally used to evaluate the global accuracy of the model.

Precision rate (precision) indicates how many of the predicted positive samples are real positive samples. Recall rate (recall) is the proportion of all positive samples correctly identified as positive samples. For a binary classification problem, there are

$$Precision = TP/(TP + \mathrm{FP}) \tag{14}$$

$$Recall = TP/(TP + \mathrm{FN}) \tag{15}$$

where FP is the number of samples that are classified as positive in the negative samples, FN is the number of samples that are classified as negative in the positive samples.

F1-score (F1) is the harmonic mean value of precision and recall [31], which is calculated according to the expression

$$F1 = (2 \times \mathrm{Pr} \times Re)/(\mathrm{Pr} + \mathrm{Re}) \tag{16}$$

where Pr and Re are respectively referring to precision and recall. F1-score can comprehensively evaluate the recognition effect of the model.

Multi-classification problems are often transformed into binary classification problems to calculate the precision, recall, and F1-score of a specific class step by step.

B. FIRST-STEP TRANSFER LEARNING

In the framework of the method proposed, the first-step transfer mainly solves the problem of model training speed and efficiency, and lays the foundation for the second-step transfer. The target domain of first-step transfer is the simulated

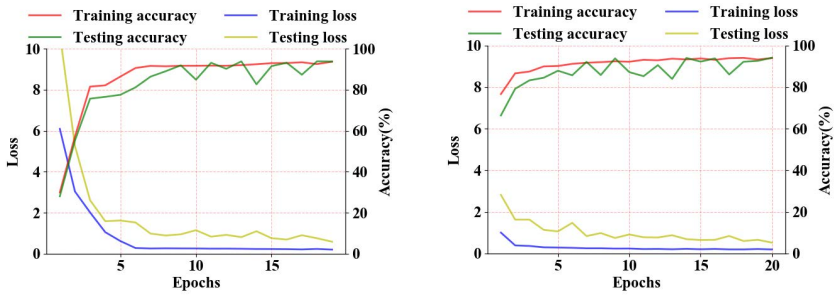

FIGURE 8. Comparison of the two learning modes (first-step transfer). (a) The result of learning from scratch. (b) The result of deep transfer learning (the training dataset is the simulated dataset).

range-Doppler images, whose generation method is introduced in Section 3.1. During the experiment, the training set and the test set were divided at 8:2 ratio. The typical Resnet18 model is used, the hyperparameters are set as learning rate is automatic, the batch size is selected as 16, the number of training epochs is set as 30. The training set data is input into the model, and the learning from scratch and transfer learning methods are used for training and comparison. The change in the cross-entropy loss value and recognition accuracy of the network model with the number of iterations is shown in Fig.8.

During learning from scratch, it can be seen that as the number of training epochs increases, the training and testing accuracy rates increase. After nine epochs of training, the training accuracy finally reaches 95.73%, and the testing accuracy is about 93.01%. No matter the training loss or testing loss, they all gradually decrease with the increase of the number of training epochs. When the network hyperparameter settings remain same as the learning from scratch, the deep transfer learning model in Section 3.3 is adopted and the dataset established in Section 3.1 is used to train the model. It's shown that the recognition accuracy and loss change with the number of training epochs as shown in Fig.8(b).

It can be seen that the training accuracy has reached 90.13% at the second epoch of training. After five epochs of training, the training accuracy has reached 94.56%, and the testing accuracy is about 92.90%, which are near the training effect of the learning from scratch at the ninth epoch. The training loss and testing loss all gradually decrease with the increase of the number of training epochs.

The final recognition accuracy of the two training methods is not much different. The training method based on transfer learning converges faster than learning from scratch, and the time to achieve the same recognition effect nearly is 0.5 times that of learning from scratch.

C. SECOND-STEP TRANSFER LEARNING

In the framework of this paper method, the second-step of deep transfer learning is mainly to improve the recognition accuracy. The network model obtained by first-step transfer is used as a pre-training model for second-step transfer, so as to improve the accuracy of multi-aircraft formation recognition. In the experiment, the first thing we do is data augmentation. The training set and test set division and model hyperparameter settings are the same as in the previous section. Then, the learning from scratch and transfer learning methods are used for training and comparison. The changes in the cross-entropy loss value and recognition accuracy of the network model with the number of epochs are shown in Fig.9.

In the process of fine-tuning the network model obtained by the first-step transfer, it can be seen that the testing accuracy has gradually increased from 85.6% to 94.9%. The testing loss gradually decreases with the number of epochs. In the finally, the testing accuracy and loss are all very close to the training values. Fig.9(b) shows the change in the recognition accuracy and loss of the learning from scratch with the number of epochs. We can see that the training accuracy quickly increased to more than 90%, but the testing accuracy increased slowly with the number of epochs, and the oscillation was violent. The maximum recognition accuracy rate only is 86%. The loss gradually decreased with the epochs, and the oscillation was also violent. This is because the size of real measured data is small, and when learning from scratch, it is easy to overfit, resulting in the result of high training accuracy but low testing accuracy.

We plot the confusion matrices resulting from the recognition of the two learning modes. In Fig.10, it can be seen that when mode learning from scratch is adopted, the recognize effects of category 2 and category 4 are very low. The model obtained by the transfer learning training has a relatively balanced recognition effect for each category, and the recognition effect of category 2 and category 4 has been greatly improved.

By calculating the precision, recall, and F1-score of the models trained in the two modes, we can obtain the result in Table.1.

From the comparison of the evaluation indicators in Table.1, it can be seen that the F1-score is significantly higher in the second-step transfer than the learning from scratch, that

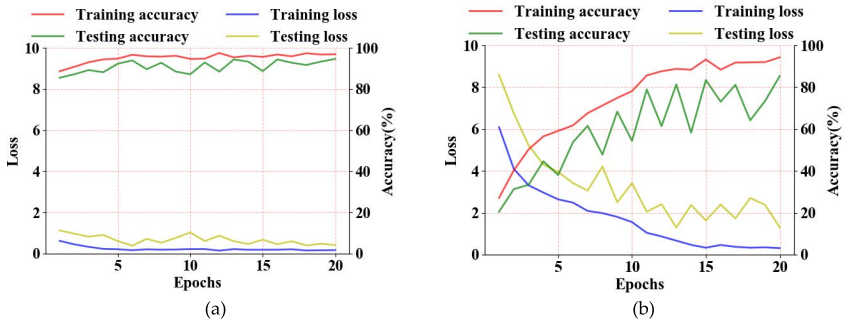

FIGURE 9. Comparison of the two learning modes (second-step transfer). (a) The result of deep transfer learning (the training dataset is the real measured dataset). (b) The result of learning from scratch.

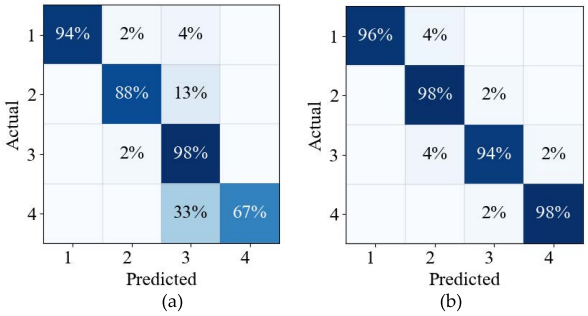

FIGURE 10. Confusion matrices of the two learning modes. (a) The result of learning from scratch. (b) The result of deep transfer learning.

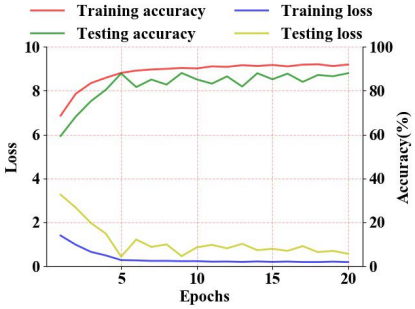

FIGURE 11. The result of one-step deep transfer learning.

TABLE 1. Comparison of the two learning modes.

Mode	Class	Precision / %	Recall / %	F1 / %	Accuracy / %
Learning from scratch	Class 1	100	93	96	86%
	Class 2	95	87	91	
	Class 3	65	97	78	
	Class 4	100	66	79	
Deep transfer learning	Class 1	100	95	97	95%
	Class 2	92	97	95	
	Class 3	95	93	94	
	Class 4	97	97	97	

is, the model obtained by the second-step transfer learning has strong recognition ability and good effect.

When we adopt the ImageNet dataset as the source domain and the real measured dataset as the target domain, the transfer process is a one-step transfer. The result of the one-step transfer experience is shown in Fig.11. We can see that the best testing accuracy only reaches 87.8%, which is far lower than the second-step transfer result shown in Fig. 9(a).

Compared with one-step deep transfer learning, the two-step deep transfer learning proposed in this paper has stronger practicability under the condition of a small sample size.

D. COMPARATION WITH THE TRADITIONAL CFAR

To test the effect of the proposed method, we compare it with the typical CA-CFAR detection method.

Fig.12(a) is a simulated range-Doppler image including three multi-aircraft formations. At the distance of 895 km, there is an aircraft formation of two targets, of which Doppler frequencies are 21 and 23 respectively. At the distance of 980 km, there is an aircraft formation of three aircrafts. Their Doppler frequencies are -16, -17, and -18. At the distance of 1180 km, there is an aircraft formation of two aircraft targets with Doppler frequency of 17 and 18. Fig.12(b) is a simulated range-Doppler image including two multi-aircraft formations with multipath effect. At the distance of 920 km, there is an aircraft formation of two targets, of which Doppler frequencies are 21 and 23 respectively. At the distance of 990 km, there is an aircraft formation of two aircrafts. Their Doppler frequencies are -19 and -21.

By using the classic CA-CFAR detection method, when $P_{fa} = 10^{-6}$, the target detection effect is shown in Fig.13. As can be seen from Fig.13, all of the aircraft formations are incorrectly judged as only one target. To achieve effective recognition of multi-aircraft formation, it is necessary to reduce the detection threshold and increase the probability of false alarms, so that interference, clutter, and outliers cannot be effectively eliminated, which made the performance of the CFAR processor became lower. When $P_{fa} = 10^{-5}$, the detection effect of the target is shown in Fig.14. It can

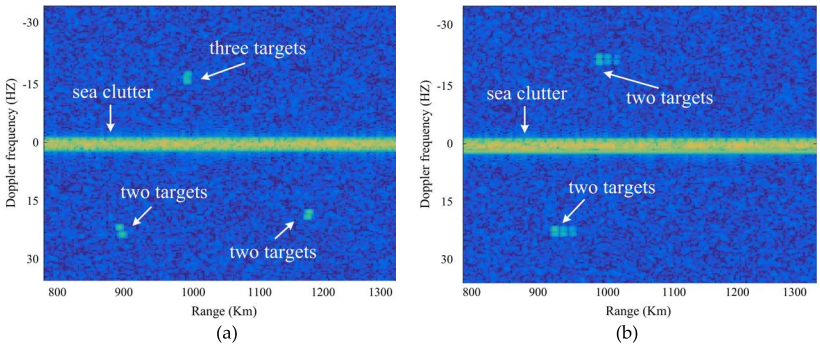

FIGURE 12. Range-Doppler image including multi-aircraft formation. (a) The image including three multi-aircraft formations. (b) The image including two multi-aircraft formations with multipath effect.

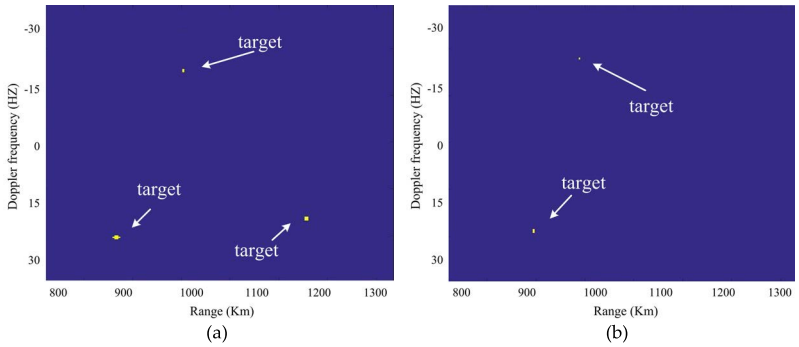

FIGURE 13. Detection effect of CA-CFAR detection method (when $P_{fa} = 10^{-6}$). (a) The image including three multi-aircraft formations. (b) The image including two multi-aircraft formations with multipath effect.

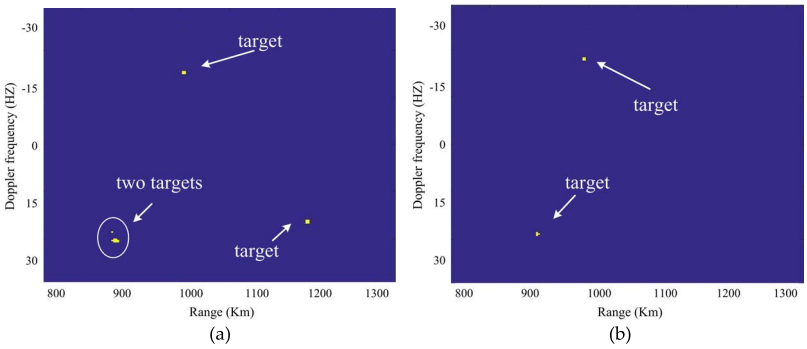

FIGURE 14. Detection effect of CA-CFAR detection method (when $P_{fa} = 10^{-5}$). (a) The image including three multi-aircraft formations. (b) The image including two multi-aircraft formations with multipath effect.

be seen from Fig.14(a) that two aircraft formations at distance of 980 km and 1180 km couldn't be recognized, and only a batch of two targets at distance of 895 km is correctly detected. In the Fig.14(b), all of multi-aircraft formation are recognized as one aircraft. We continue to adjust the false alarm rate, when $P_{fa} = 10^{-3}$, the detection effect of the target is shown in Fig.15. As can be seen from the Fig.15(a), two aircraft formations are correctly detected. But at the same time, two noises were falsely detected as 'targets', and a two-aircraft formation were falsely detected as one aircraft. In the Fig.15(b), only one multi-aircraft formation is correctly detected. But at the same time, one noises were falsely detected as 'targets' and a two-aircraft formation were falsely detected as three-aircraft formation because of multipath effect. It's shown that multi-aircraft formation recognition through traditional CFAR detection is very difficult.

By using the proposed method of this paper, when $P_{fa} = 10^{-6}$, we can see from Fig.16 that all multi-aircraft formations are accurately detected.

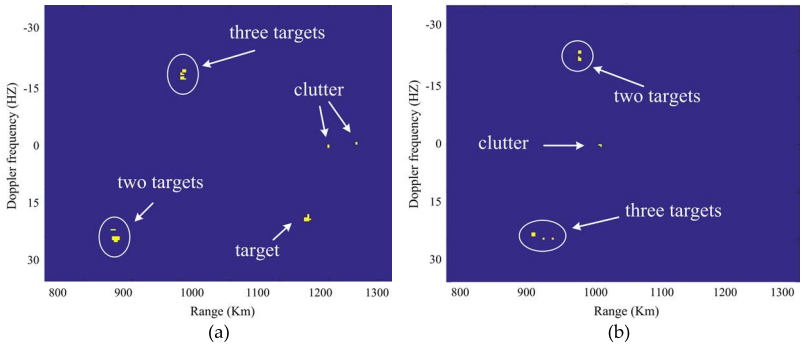

FIGURE 15. Detection effect of CA-CFAR detection method (when $P_{fa} = 10^{-3}$). (a) The image including three multi-aircraft formations. (b) The image including two multi-aircraft formations with multipath effect.

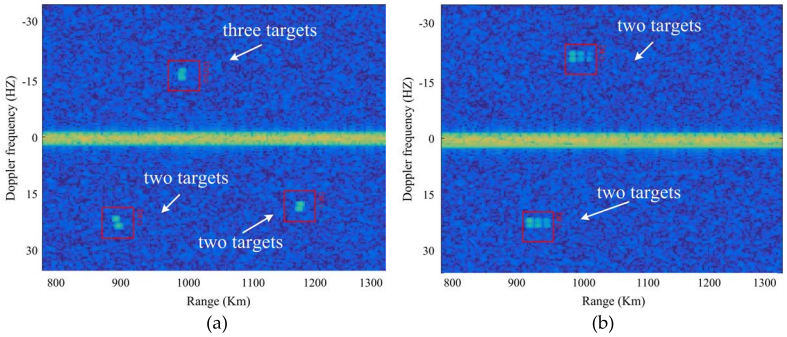

FIGURE 16. Detection effect using the proposed method. (a) The image including three multi-aircraft formation. (b) The image including two multi-aircraft formation with multipath effect.

When it comes to target recognition, the recognition speed is very important. The faster recognition speed of the model is, the better recognition ability of the model is [32]. Because the recognition model is usually trained in the spare time, it is of no practical significance to discuss the training time, which is why we only discuss the classification time of the model using different deep learning networks. As we all know, the classification time of CNN is affected by the complexity of the network structure, the input image size, computing power, and so on. We adopt the CA-CFAR as the CFAR detector and use the different CNN models to recognize the detected result. Under the same computational power and input image size, we compared the classification time and recognition accuracy of the different models.

As shown in Fig.17, when only using CA-CFAR to recognize the formation target, the classification time is 0.0311 s, and the recognition accuracy is 39.0%.

After adding the deep learning network to the model, such as VGG16, Inception-V3, ResNet18, and so on [33], the recognition accuracies all pass 90.0%, and the classification time is only 1 to 5 milliseconds longer than that of CA-CFAR. The proposed method CA-CFAR + ResNet18 has a lower classification time than those of CA-CFAR + VGG16, CA-CFAR + Inception-V3 and CA-CFAR + MobileNet-V2 and higher recognition accuracy than all other methods.

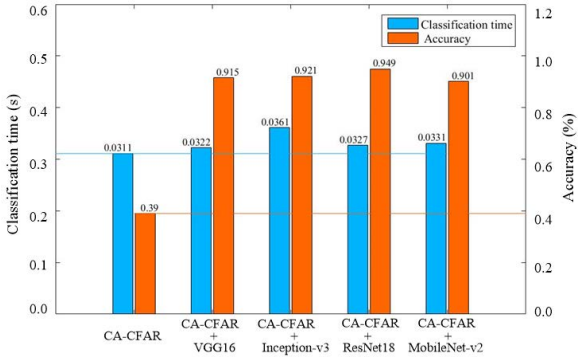

FIGURE 17. The classification time and the accuracy comparison of the different models in the proposed recognition method under the same condition.

The above comparison with the traditional CA-CFAR processor shows the superiority of the proposed method in multi-aircraft formation recognition.

V. CONCLUSION

In this paper, a recognition method of multi-aircraft formation of OTHR based on deep transfer learning is proposed. After experimental verification, the following conclusions are drawn.

1) The designed recognition model combining CNN and CFAR has greatly enhanced the recognition ability of multi-aircraft formation compared with the traditional CFAR detection method, especially for multi-aircraft formation with multipath effect.
2) The model training method of two-step transfer greatly improves the performance of the model compared with learning from scratch. In the recognition of four classes of targets, the accuracy of the model is 95%, which is 9% higher than learning from scratch.
3) The simulation and data expansion of multi-target formation are effective, which solves the problem that it is difficult to apply deep learning technology due to the lack of real measured data.

However, we should recognize the limitation of the proposed method, that is, the method is mainly affected by the setting parameter and the detection ability of the radar. If the resolution of range-Doppler image generated by radar is too low, the recognition results will be poor.

In the future work, in addition to improving the recognition accuracy of the model continuously, we will explore the end-to-end method for aircraft formation recognition by using deep detectors such as YOLO, SSD, and so on, and will establish an end-to-end deep learning framework to predict and trace the aircraft formation.

REFERENCES

[1] T. Thayaparan, Y. Ibrahim, J. Polak, and R. Riddolls, "High-frequency over-the-horizon radar in Canada," *IEEE Geosci. Remote Sens. Lett.*, vol. 15, no. 11, pp. 1700–1704, Nov. 2018.
[2] K. Zebiri and A. Mezache, "Radar CFAR detection for multiple-targets situations for Weibull and log-normal distributed clutter," *Signal, Image Video Process.*, vol. 15, no. 8, pp. 1671–1678, Apr. 2021.
[3] M. Liu, C. Wang, H. Zeng, and C. Zhou, "Effect of dual aircraft formation spacing on target position tracking on measurement conversion by monopulse radar," *AIP Adv.*, vol. 11, no. 7, Jul. 2021, Art. no. 075326.
[4] S. J. Davey, G. A. Fabrizio, and M. G. Rutten, "Detection and tracking of multipath targets in over-the-horizon radar," *IEEE Trans. Aerosp. Electron. Syst.*, vol. 55, no. 5, pp. 2277–2295, Oct. 2019.
[5] J. Zhao, R. Jiang, X. Wang, and H. Gao, "Robust CFAR detection for multiple targets in K-distributed sea clutter based on machine learning," *Symmetry*, vol. 11, no. 12, p. 1482, Dec. 2019.
[6] J. Cai, S. Hu, Y. Jin, J. Mo, T. Yan, and M. Xia, "A CA-CFAR-Like detector using the Gerschgorin circle theorem for bistatic space based radar," *IEEE Trans. Aerosp. Electron. Syst.*, vol. 57, no. 6, pp. 4137–4148, Dec. 2021.
[7] A. Abbadi, H. Bouhedjeur, A. Bellabas, T. Menni, and F. Soltani, "Generalized closed-form expressions for CFAR detection in heterogeneous environment," *IEEE Geosci. Remote Sens. Lett.*, vol. 15, no. 7, pp. 1011–1015, Jul. 2018.
[8] T. Li, Z. Liu, R. Xie, and L. Ran, "An improved superpixel-level CFAR detection method for ship targets in high-resolution SAR images," *IEEE J. Sel. Topics Appl. Earth Observ. Remote Sens.*, vol. 11, no. 1, pp. 184–194, Jan. 2018.
[9] Y. Liu, S. Zhang, J. Suo, J. Zhang, and T. Yao, "Research on a new comprehensive CFAR (Comp-CFAR) processing method," *IEEE Access*, vol. 7, pp. 19401–19413, 2019.
[10] Y. Fan, M. Tao, J. Su, and L. Wang, "Weak target detection based on joint fractal characteristics of autoregressive spectrum in sea clutter background," *IEEE Geosci. Remote Sens. Lett.*, vol. 16, no. 12, pp. 1824–1828, Dec. 2019.
[11] J. Ai, R. Tian, Q. Luo, J. Jin, and B. Tang, "Multi-scale rotation-invariant Haar-like feature integrated CNN-based ship detection algorithm of multiple-target environment in SAR imagery," *IEEE Trans. Geosci. Remote Sens.*, vol. 57, no. 12, pp. 10070–10087, Dec. 2019.
[12] X. Bi, J. Du, Q. Zhang, and W. Wang, "Improved multi-target radar TBD algorithm," *J. Syst. Eng. Electron.*, vol. 26, no. 6, pp. 1229–1235, Dec. 2015.
[13] L. Wang, W. Zhu, Y. Zhang, Q. Liao, and J. Tang, "Multi-target detection and adaptive waveform design for cognitive MIMO radar," *IEEE Sensors J.*, vol. 18, no. 24, pp. 9962–9970, Dec. 2018.
[14] E. Tavanti, A. Rizik, A. Fedeli, D. D. Caviglia, and A. Randazzo, "A short-range FMCW radar-based approach for multi-target human-vehicle detection," *IEEE Trans. Geosci. Remote Sens.*, vol. 60, pp. 1–16, 2022.
[15] S. Hong, S. Lee, B.-H. Lee, J. Kim, Y.-H. Kim, and S.-C. Kim, "Radar signal decomposition in steering vector space for multi-target classification," *IEEE Sensors J.*, vol. 21, no. 22, pp. 25843–25852, Nov. 2021.
[16] A. Testolin and R. Diamant, "Combining denoising autoencoders and dynamic programming for acoustic detection and tracking of underwater moving targets," *Sensors*, vol. 20, no. 10, p. 2945, May 2020.
[17] W. Kim, H. Cho, J. Kim, B. Kim, and S. Lee, "YOLO-based simultaneous target detection and classification in automotive FMCW radar systems," *Sensors*, vol. 20, no. 10, p. 2897, May 2020.
[18] Q. Gao, S. Jiang, and P. B. Shull, "Simultaneous hand gesture classification and finger angle estimation via a novel dual-output deep learning model," *Sensors*, vol. 20, no. 10, p. 2972, May 2020.
[19] B. Maschler, S. Kamm, N. Jazdi, and M. Weyrich, "Distributed cooperative deep transfer learning for industrial image recognition," *Proc. CIRP*, vol. 93, pp. 437–442, Jun. 2020.
[20] T. Theurer and W. Bristow, "High-latitude OTHR adaptive beamforming: Preserving angle-Doppler coupled clutter," *IEEE Trans. Aerosp. Electron. Syst.*, vol. 56, no. 4, pp. 3149–3161, Aug. 2020.
[21] L. Han, Y. Zhao, H. Chen, and V. Chandrasekar, "Advancing radar nowcasting through deep transfer learning," *IEEE Trans. Geosci. Remote Sens.*, vol. 60, pp. 1–9, 2022.
[22] X. Yang, Y. Zhang, W. Lv, and D. Wang, "Image recognition of wind turbine blade damage based on a deep learning model with transfer learning and an ensemble learning classifier," *Renew. Energy*, vol. 163, pp. 386–397, Jan. 2021.
[23] M. A. Khan, T. Akram, Y.-D. Zhang, and M. Sharif, "Attributes based skin lesion detection and recognition: A mask RCNN and transfer learning-based deep learning framework," *Pattern Recognit. Lett.*, vol. 143, pp. 58–66, Mar. 2021.
[24] F. Zhuang, Z. Qi, K. Duan, D. Xi, Y. Zhu, H. Zhu, H. Xiong, and Q. He, "A comprehensive survey on transfer learning," *Proc. IEEE*, vol. 109, no. 1, pp. 43–76, Jan. 2021.
[25] C. Tan, F. Sun, T. Kong, W. Zhang, C. Yang, and C. Liu, "A survey on deep transfer learning," in *Proc. 27th Int. Conf. Artif. Neural Netw. (ICANN)*, vol. 11141, Oct. 2018, pp. 270–279.
[26] Z. Huang, Z. Pan, and B. Lei, "What, where, and how to transfer in SAR target recognition based on deep CNNs," *IEEE Trans. Geosci. Remote Sens.*, vol. 58, no. 4, pp. 2324–2336, Apr. 2019.
[27] X. Zhao, Y. Liang, A. J. X. Guo, and F. Zhu, "Classification of small-scale hyperspectral images with multi-source deep transfer learning," *Remote Sens. Lett.*, vol. 11, no. 4, pp. 303–312, Apr. 2020.
[28] S.-Z. Shi, Z.-Y. Zhao, Y. Liu, G. Chen, T. Li, J.-N. Liu, and M. Yao, "Experimental demonstration for ionospheric sensing and aircraft detection with a HF skywave multistatic radar," *IEEE Geosci. Remote Sens. Lett.*, vol. 11, no. 7, pp. 1270–1274, Jul. 2014.
[29] Y. Huang, Y. Shi, and T. Song, "An efficient multi-path multitarget tracking algorithm for over-the-horizon radar," *Sensors*, vol. 19, no. 6, p. 1384, Mar. 2019.
[30] X. Zhang, Z. Wang, D. Liu, Q. Lin, and Q. Ling, "Deep adversarial data augmentation for extremely low data regimes," *IEEE Trans. Circuits Syst. Video Technol.*, vol. 31, no. 1, pp. 15–28, Jan. 2021.
[31] Z. Yu, J. Tang, and Z. Wang, "GCPS: A CNN performance evaluation criterion for radar signal intrapulse modulation recognition," *IEEE Commun. Lett.*, vol. 25, no. 7, pp. 2290–2294, Jul. 2021.
[32] M. Amrani and F. Jiang, "Deep feature extraction and combination for synthetic aperture radar target classification," *J. Appl. Remote Sens.*, vol. 11, no. 4, Oct. 2021, Art. no. 042616.
[33] M. Amrani, F. Jiang, Y. Xu, S. Liu, and S. Zhang, "SAR-oriented visual saliency model and directed acyclic graph support vector metric based target classification," *IEEE J. Sel. Topics Appl. Earth Observ. Remote Sens.*, vol. 11, no. 10, pp. 3794–3810, Oct. 2018.

FUTAI LIANG received the master's degree in information and communication engineering from the Air Force Early Warning Academy, Wuhan, China, in 2020, where he is currently pursuing the Ph.D. degree in information and communication engineering.

His research interests include target detection, image recognition, and AI.

YAN ZHOU received the Ph.D. degree in control science and engineering from the Huazhong University of Science and Technology, Wuhan, China, in 2000.

He is currently a Professor with the Air Force Early Warning Academy, Wuhan. His research interests include pattern recognition, data fusion, and image processing.

HUI LI received the M.S. degree from the Beijing University of Technology, in 2007.

She is currently a Professor with Air Force Early Warning Academy, Wuhan. Her research interests include target tracking and multi-source information fusion.

XUN FENG received the Ph.D. degree in information and communication engineering from Air Force Early Warning Academy, Wuhan, China, in 2008.

He is currently a Lecturer with Air Force Early Warning Academy. His research interests include machine-learning and data analysis.

JUNBIAO ZHANG received the B.S. degree from the Xi'an University of Science and Technology, in 2016, and the M.S. degree from the Army Academy of Artillery and Air Defense, in 2018. He is currently pursuing the Ph.D. degree with the Air Force Early Warning Academy. His research interests include target detection and tracking and trajectory prediction.